

# The Nature of Interactions in the Ionic Crystal of 3-Pentenitrile, 2-Nitro-5-oxo, Ion(−1), Sodium

Robert W. Gora,<sup>†</sup> W. Andrzej Sokalski,<sup>†</sup> Jerzy Leszczynski,<sup>\*,‡</sup> and Virginia B. Pett<sup>§</sup>

Molecular Modeling Laboratory, Institute of Physical and Theoretical Chemistry, I-30, Wrocław University of Technology, Wyb. Wyspiańskiego 27, 50-370 Wrocław, Poland, Computational Center for Molecular Structure and Interactions, Department of Chemistry, Jackson State University, Jackson, Mississippi 39217, and Department of Chemistry, The College of Wooster, 943 College Mall, Wooster, Ohio 44691

Received: July 12, 2004; In Final Form: November 8, 2004

The hybrid variation–perturbation many-body interaction energy decomposition scheme has been applied to analyze the physical nature of interactions in the ionic 3-pentenitrile, 2-nitro-5-oxo, ion(−1), sodium crystal, which can be regarded as a model for a large group of aromatic quaternary nitrogen salts. In the crystal structure the sodium ions and water molecules of adjacent unit cells form a positively charged “inorganic layer” with the sodium ions clustered together along the *ab* faces with the organic (negative) part in between. This puzzling crystal packing is due to a strong favorable interaction between the water molecule and the sodium ions and a substantial charge transfer from the carbanions that balances out the destabilizing sodium–sodium ion repulsion. Although the majority of cohesion energy of the crystal structure comes from the electrostatic interactions of ions, the resulting net stabilization also depends heavily on the nonadditive delocalization components, due to a counterbalance between the two-body delocalization and exchange effects. The estimated nonadditivity of interactions varies between 12% and 22%.

## 1. Introduction

One of the most important challenges in molecular sciences remains the theoretical prediction of the crystal structure.<sup>1–3</sup> Due to the considerable size of the systems involved, most of the crystal structure simulations are still based on the atom–atom potentials, which only rarely are derived rigorously from the first principles.<sup>4–7</sup> An additional source of errors may originate from the lack of detailed knowledge of the physical nature of the intermolecular interactions involved, which results frequently in the use of improper functional form or the reference *ab initio* data used for fitting atom–atom potentials.<sup>8</sup> The necessary information on the nature of interactions can be obtained from the applications of the intermolecular perturbation theory (IMPT)<sup>9</sup> or the symmetry adapted perturbation theory (SAPT).<sup>10</sup> However, until recently such a rigorous approach was limited to the fairly small systems due to a bottleneck of the necessary conventional calculations and storage of integrals. Currently, relatively large systems can be treated rigorously within the hybrid variational–perturbational interaction energy partitioning technique,<sup>11–13</sup> exploiting the direct integral calculation and segmented transformation schemes,<sup>14,15</sup> allowing analysis of interactions in the molecular or ionic crystals.

The ring-opening reactions of several halo-nitropyridines with base were originally investigated by Reinheimer and associates.<sup>16,17</sup> The title compound is the product of the ring-opening reaction of 2-chloro-3-nitropyridine with two equivalents of base. Recently the structure of the carbanion product of this reaction was determined.<sup>18</sup> In contrast to the carbanion from 2-chloro-5-nitropyridine, which reacts with an additional equivalent

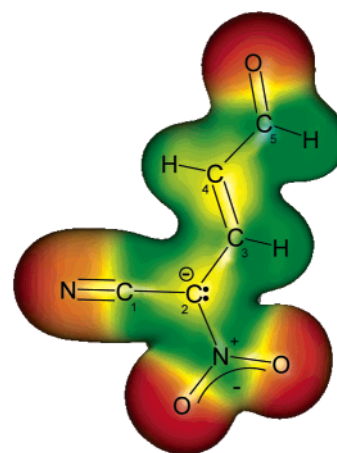


**Figure 1.** Schematic diagram of the carbanion superimposed with the electrostatic potential map calculated on the 0.02 electron/bohr<sup>3</sup> isodensity contour. The colors correspond to the values of the electrostatic potential and range from the most negative, red (−0.2 au), through a less negative, yellow (−0.1 au), and neutral, green, up to a slightly positive, blue (0.1 au).

of base to reclose the ring, the carbanion shown in Figure 1 decomposes in the presence of base to form sodium formate and sodium isocyanate.<sup>17</sup> In this paper we investigate the nature of interactions within the crystal structure of this carbanion product.

In the aforementioned crystal structure the sodium ions and water molecules of adjacent unit cells form a positively charged “inorganic layer” along the *ab* faces with the organic (negative) part in between. Although it is not unusual to encounter like ions (sodium, calcium ions, for example) organized inside crystals into single or even double sheets,<sup>19</sup> the fact that despite the electrostatic repulsion between the positive charges the

\* Corresponding author. Tel: (601) 979-7824. Fax: (601) 979-7823. E-mail: jerzy@ccmsi.us.

<sup>†</sup> Wrocław University of Technology.

<sup>‡</sup> Jackson State University.

<sup>§</sup> The College of Wooster.

sodium ions are clustered together is apparently counterintuitive. Therefore one of the main objectives of this study was finding an explanation of this puzzling crystal packing.

## 2. Details of the Theoretical Treatment

**2.1. Interaction Energy and Difference Density Partitioning Schemes.** The many-body effects may sometimes be contributions of great importance, especially in the case of charged systems.<sup>20–24</sup> Therefore in this work we will use the following partitioning technique in order to investigate these effects thoroughly.

In the supermolecular approach the total interaction energy of an  $n$ -fragment system can be partitioned into 2-, 3-, ...,  $n$ -body components as follows:<sup>15,25–27</sup>

$$\Delta E = E(12\dots n) - \sum_{I=1}^n E(I) = \sum_{I=1}^{n-1} \sum_{J>I}^n \Delta^2 E(IJ) + \sum_{I=1}^{n-2} \sum_{J>I}^{n-1} \sum_{K>J}^n \Delta^3 E(IJK) + \dots + \Delta^n E(12\dots n) \quad (1)$$

The first summation runs over all monomers, the second over all dimers, etc.  $E(I)$ ,  $E(IJ)$ , ..., are the total energies of monomers, dimers, etc., whereas  $\Delta^2 E(IJ)$ ,  $\Delta^3 E(IJK)$ , etc., are the individual two-, three-, and higher-order many-body contributions to the interaction energy (eqs 2 and 3).

$$\Delta^2 E(IJ) = E(IJ) - \sum_{I=1}^2 E(I) \quad (2)$$

$$\Delta^3 E(IJK) = E(IJK) - \sum_{I=1}^3 E(I) - \sum_{I=1}^2 \sum_{J>I}^3 \Delta^2 E(IJ) \quad (3)$$

We will use the term “nonadditive” interchangeably with “many-body” referring to 3-, 4-, and higher-order  $n$ -body contributions to the interaction energy or its components.

In this work we will utilize eq 1 in partitioning the interaction energies calculated at the Møller–Plesset second-order perturbation theory level (MP2).<sup>28</sup> In all the necessary calculations the complex-centered basis set (CCBS) was utilized. Such a procedure corresponds to the site–site function counterpoise (SSFC) method of basis set superposition error (BSSE) correction<sup>29</sup> (a recent discussion of the subject can be found in a paper by Mierzwicki et al.<sup>30</sup>). The total MP2 interaction energy of an  $n$ -fragment system can be expressed as follows:<sup>31,32</sup>

$$\Delta E^{MP2} = \sum_{i=0}^2 \epsilon_{MP}^{(i)} = \Delta E^{HF} + \epsilon_{MP}^{(2)} \quad (4)$$

where  $\Delta E^{HF}$  is the interaction energy obtained in the supermolecular approach from the restricted Hartree–Fock energies of subsystems, whereas  $\epsilon_{MP}^{(2)}$  encompasses the electron correlation corrections to this interaction calculated accordingly. The Hartree–Fock interaction energy can be partitioned into the first-order Heitler–London and the higher-order Hartree–Fock delocalization components.

$$\Delta E^{HF} = \Delta E^{HL} + \Delta E_{del}^{HF} \quad (5)$$

The Heitler–London interaction energy encompasses the first-order electrostatic interactions between all 1, 2, ...,  $n$  monomers and the associated Heitler–London exchange repulsion due to

the Fermi electron correlation effects.<sup>33</sup> It is calculated after Löwdin<sup>34</sup> as

$$\Delta E^{HL} = N_{12\dots n}^{HL} \langle \hat{A} \prod_{I=1}^n \Psi_I | \hat{H}_{12\dots n} | \hat{A} \prod_{I=1}^n \Psi_I \rangle - \sum_{I=1}^n E^{HF}(I) \quad (6)$$

In the above expression  $\hat{A}$  is the standard antisymmetrizer,  $\Psi_I$  are the HF wave functions of the isolated monomers, and  $N_{12\dots n}^{HL}$  is the appropriate normalization constant. The Hamiltonian in eq 6 is defined as a sum of the free-monomer Hamiltonians and the intermolecular perturbation  $\hat{V}$ .

$$\hat{H}_{12\dots n} = \sum_{I=1}^n \hat{H}_I + \hat{V} \quad (7)$$

Taking into account the fact that the first-order electrostatic interaction is pairwise additive, it can be calculated as

$$\epsilon_{el}^{(10)} = \sum_{I=1}^{n-1} \sum_{J>I}^n \epsilon_{el}^{(10)}(IJ) \quad (8)$$

where the  $\epsilon_{el}^{(10)}(IJ)$  term can be calculated from the following perturbational expression, assuming that the complex-centered basis set has been applied:

$$\epsilon_{el}^{(10)}(IJ) = \sum_{pq} d_{pq}^I n_{pq}^J + \sum_{rs} d_{rs}^J n_{rs}^I + \sum_{pqrs} d_{pq}^I d_{rs}^J g_{pqrs} + V_{NN}^{IJ} \quad (9)$$

( $n$ ,  $g$ , and  $\mathbf{d}$  are respectively the potential and two-electron atomic integrals and the corresponding one-electron density matrices of monomers  $I$  and  $J$ , whereas  $V_{NN}^{IJ}$  is the  $I$ – $J$  nuclear repulsion; the  $p$ ,  $q$ ,  $r$ ,  $s$  indices span over the entire atomic orbital basis of the complex).<sup>12</sup> The Heitler–London exchange repulsion is therefore given by<sup>11</sup>

$$\epsilon_{ex}^{HL} = \Delta E^{HL} - \epsilon_{el}^{(10)} \quad (10)$$

The  $\epsilon_{ex}^{HL}$  component can be further partitioned into the two-body exchange repulsion

$$\epsilon_{ex,2}^{HL} = \sum_{I=1}^{n-1} \sum_{J>I}^n \epsilon_{ex}^{HL}(IJ) \quad (11)$$

and the many-body exchange effects given by the nonadditive Heitler–London components obtained by partitioning  $\Delta E^{HL}$  according to eq 1. Essentially the  $\epsilon_{el}^{(10)}(IJ)$  term can also be divided into the short-range penetration  $\epsilon_{el,PEN}^{(1)}$  and the long-range multipolar  $\epsilon_{el,DMA}^{(1)}$  component, calculated from the finite, distributed multipolar expansions based on numerically equivalent spherical-harmonic<sup>35,36</sup> or Cartesian formulations.<sup>37,38</sup> The delocalization component

$$\Delta E_{del}^{HF} = \Delta E^{HF} - \Delta E^{HL} \quad (12)$$

which gathers collectively the effects associated with the relaxation of the electronic densities of monomers upon interaction restrained by the Pauli exclusion principle,<sup>39</sup> can be partitioned in a manner similar to the exchange repulsion into 2-, 3-, ...,  $n$ -body components, since the many-body delocalization effects are given by the difference between the  $\Delta E^{HF}$  and  $\Delta E^{HL}$  nonadditivity. Therefore, the total counterpoise-corrected Hartree–Fock interaction energy can be partitioned as follows:

$$\Delta E^{HF} = \epsilon_{el}^{(10)} + \epsilon_{ex,2}^{HL} + \epsilon_{ex,3}^{HL} + \dots + \epsilon_{ex,n}^{HL} + \Delta E_{del,2}^{HF} + \Delta E_{del,3}^{HF} + \dots + \Delta E_{del,n}^{HF} \quad (13)$$

The electron correlation  $\epsilon_{MP}^{(2)}$  term can also be partitioned in a similar fashion. This term incorporates the second-order dispersion interaction due to the intermolecular Coulomb electron correlation effects<sup>40</sup>

$$\epsilon_{disp}^{(20)}(IJ) = 4 \sum_{i \in I} \sum_{j \in J} \sum_{a \in I} \sum_{b \in J} \frac{\langle ij|ab \rangle \langle ab|ij \rangle}{\epsilon_j - \epsilon_a - \epsilon_b} \quad (14)$$

( $i, j$ , and  $a, b$  are the occupied and virtual molecular orbitals of monomers  $I$  and  $J$ , respectively) and the electron correlation corrections to the Hartree–Fock components. The correlation correction to the first-order electrostatic interaction can be evaluated from the following formula, assuming the complex-centered basis set has been applied:

$$\epsilon_{el,r}^{(12)}(IJ) = \sum_{pq} d_{pq}^{(02),I} n_{pq}^J + \sum_{pq} d_{pq}^{(02),J} n_{pq}^I + \sum_{pqrs} (d_{pq}^{(02),J} d_{rs}^I + d_{pq}^{(02),I} d_{rs}^J) g_{pqrs} \quad (15)$$

where  $\mathbf{d}^{(02)}$  are the so-called relaxed density matrices of monomers  $I$  and  $J$ .<sup>41</sup> Since the second-order dispersion and electrostatic contributions are pairwise additive, the total  $\epsilon_{el,r}^{(12)}$  and  $\epsilon_{disp}^{(20)}$  interaction energy terms in an  $n$ -body system can be evaluated as

$$\epsilon_{el,r}^{(12)} = \sum_{I=1}^{n-1} \sum_{J>I}^n \epsilon_{el,r}^{(12)}(IJ) \quad (16)$$

$$\epsilon_{disp}^{(20)} = \sum_{I=1}^{n-1} \sum_{J>I}^n \epsilon_{disp}^{(20)}(IJ) \quad (17)$$

The remaining electron correlation corrections are collectively gathered in the exchange–delocalization component  $\Delta E_{ex-del}^{(2)}$ , whose main contribution is due to the electron correlation corrections to the  $\epsilon_{ex}^{HL}$  component.

$$\Delta E_{ex-del}^{(2)} = \epsilon_{MP}^{(2)} - \epsilon_{el,r}^{(12)} - \epsilon_{disp}^{(20)} \quad (18)$$

Similarly as in the case of Heitler–London exchange and delocalization components the  $\Delta E_{ex-del}^{(2)}$  term can be partitioned into 2-, 3-, ...,  $n$ -body terms, where the many-body  $\Delta E_{ex-del}^{(2)}$  terms are evaluated as the difference between the  $\Delta E_{MP2}$  and  $\Delta E^{HF}$  nonadditive contributions. Therefore, the total counterpoise-corrected MP2 interaction energy can be partitioned as follows:

$$\Delta E^{MP2} = \Delta E^{HF} + \epsilon_{el,r}^{(12)} + \epsilon_{disp}^{(20)} + \Delta E_{ex-del,2}^{(2)} + \Delta E_{ex-del,3}^{(2)} + \dots + \Delta E_{ex-del,n}^{(2)} \quad (19)$$

The total electronic density of the 2-, 3-, ...,  $n$ -body complex can also be decomposed in a manner similar to the total energy (eq 1). Visualization of the changes in the electronic density distributions caused by the many-body interactions supplements the results of the interaction energy partitioning and can be helpful in achieving a better understanding of the origins of these effects. The resulting isodensity maps will be hereafter referred to as the total or  $n$ -body interaction difference density maps (IDDM).

**2.2. Details of Calculations.** In all calculations reported in this work, we have assumed the experimentally determined crystal structure.<sup>18</sup> The results reported in this work were obtained using two split valence polarized basis sets. They include the 3-21G basis set supplemented with d-type polariza-

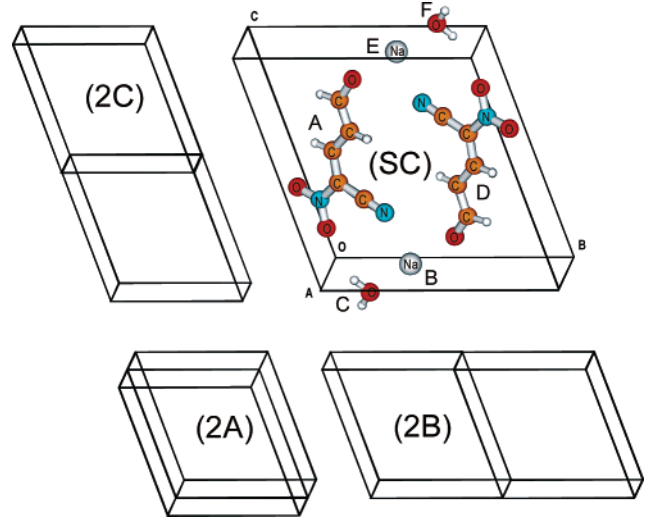


**Figure 2.** Super-cell (SC) structure of the investigated ionic crystal and a schematic representation of the selected systems studied in this work (2A, 2B, 2C). The letters A–F are used to label the interacting subsystems within the super-cell.

**TABLE 1: Results of Many-Body Partitioning of the Super-Cell Interaction Energy<sup>a</sup>**

	3-21G(d,p)	6-31G(d,p)	cc-pVDZ
$\epsilon_{el}^{(10)}$	−290.1	−279.5	−277.8
$\epsilon_{el,DMA}^{(1)}$	−294.0	−275.0	−273.0
$\epsilon_{el,PEN}^{(1)}$	3.9	−4.5	−4.7
$\epsilon_{ex,2}^{HL}$	33.2	33.3	32.4
$\epsilon_{ex,3+}^{HL}$	0.0	0.0	0.0
$\Delta E_{del,2}^{HF}$	−48.8	−52.9	−50.8
$\Delta E_{del,3}^{HF}$	37.3	38.8	37.9
$\Delta E_{del,4}^{HF}$	−4.5	−4.7	−4.6
$\Delta E_{del,5+}^{HF}$	0.2	0.2	0.2
$\Delta E^{HF}$	−272.8	−264.9	−262.6
$\Delta E_2^{HF}$	−305.7	−299.1	−296.1
$\Delta E_3^{HF}$	37.3	38.7	37.9
$\Delta E_4^{HF}$	−4.5	−4.7	−4.6
$\Delta E_{5+}^{HF}$	0.2	0.2	0.2
$\epsilon_{el,r}^{(12)}$		1.5	2.1
$\epsilon_{disp}^{(20)}$		−6.1	−5.6
$\Delta E_{ex-del,2}^{(2)}$		0.9	0.9
$\Delta E_{ex-del,3}^{(2)}$		6.0	6.0
$\Delta E_{ex-del,4+}^{(2)}$		−1.6	−1.5
$\epsilon_{MP}^{(2)}$		0.7	1.8
$\epsilon_{MP,2}^{(2)}$		−3.7	−2.6
$\epsilon_{MP,3}^{(2)}$		6.0	6.0
$\epsilon_{MP,4+}^{(2)}$		−1.6	−1.5

<sup>a</sup> Subscript “+” indicates the sum of all remaining many-body terms. All values are in kcal/mol.

tion functions on the second-row atoms and p-type polarization functions on hydrogens denoted as 3-21G(d,p)<sup>42–44</sup> and the standard 6-31G(d,p)<sup>45–47</sup> basis sets. Such a choice was due to the size of the systems taken into consideration ranging from 34 to 136 atoms and the complexity of necessary calculations. The largest calculations required evaluation of the restricted Hartree–Fock wave functions for 301 subsystems with 1144 basis functions in the 3-21G(d,p) basis set. To determine the general trends of the influence of basis set extension on the interaction energy components, we compared the performance of the selected basis sets with the results obtained in the correlation consistent cc-pVTZ basis set in the case of the super-cell structure (Figure 2). The results reported in Table 1 indicate that the only component significantly affected at the Hartree–Fock level of theory is the first-order electrostatic interaction, which is overestimated by about 10 kcal/mol in the case of the 3-21G(d,p) basis set. However, it is still less than 5% apart from

**TABLE 2: Interaction Energy Components for All Possible Dimeric Subsystems Occurring in the Super-Cell<sup>a</sup>**

	AB(DE)	AE(BD)	BC(EF)	BF(CE)	CF	AD	BE	AF(CD)	AC(DF)
3-21G(d,p)									
$\epsilon_{el}^{(10)}$	-89.5	-80.1	-26.2	-0.3	0.0	58.8	36.6	2.6	0.8
$\epsilon_{el,DMA}^{(1)}$	-90.3	-81.6	-27.1	-0.3	0.0	60.5	36.6	2.7	1.1
$\epsilon_{el,PEN}^{(1)}$	0.9	1.5	0.8	0.0	0.0	-1.7	0.0	-0.2	-0.3
$\epsilon_{ex}^{HL}$	4.8	3.3	6.2	0.0	0.0	3.8	0.0	0.0	0.4
$\Delta E_{del}^{HF}$	-9.7	-10.2	-2.7	0.0	0.0	-2.8	0.0	-0.1	-0.3
$\Delta E^{HF}$	-94.3	-87.0	-22.8	-0.3	0.0	59.7	36.6	2.5	0.9
6-31G(d,p)									
$\epsilon_{el}^{(10)}$	-87.6	-78.2	-23.1	-0.2	0.0	57.3	36.6	2.1	0.3
$\epsilon_{el,DMA}^{(1)}$	-87.3	-77.8	-23.2	-0.2	0.0	59.2	36.6	2.3	0.8
$\epsilon_{el,PEN}^{(1)}$	-0.3	-0.5	0.1	0.0	0.0	-1.9	0.0	-0.2	-0.5
$\epsilon_{ex}^{HL}$	4.9	3.4	6.1	0.0	0.0	3.7	0.0	0.0	0.4
$\Delta E_{del}^{HF}$	-10.2	-10.8	-3.5	0.0	0.0	-3.0	0.0	-0.1	-0.3
$\Delta E^{HF}$	-92.9	-85.6	-20.5	-0.2	0.0	58.0	36.6	2.0	0.3
$\epsilon_{MP}^{(2)}$	0.4	-0.4	-0.1	0.0	0.0	-3.3	0.0	0.0	-0.1
$\epsilon_{el,r}^{(12)}$	0.3	1.4	-0.8	0.0	0.0	-0.6	0.0	0.1	0.2
$\epsilon_{disp}^{(20)}$	-0.2	-0.2	-0.2	0.0	0.0	-3.9	0.0	-0.1	-0.4
$\Delta E_{ex-del}^{(2)}$	0.3	-1.5	0.9	0.0	0.0	1.2	0.0	0.0	0.1
$\Delta E^{MP2}$	-92.5	-86.0	-20.5	-0.3	0.0	54.7	36.6	2.0	0.2

<sup>a</sup> The labels of dimers correspond to the symbols used in Figure 2. All values are in kcal/mol.

our best estimate and therefore does not influence the qualitative picture emerging from the interaction energy partitioning.

The most recent version of the interaction energy decomposition scheme was implemented<sup>48</sup> in the GAMESS quantum chemistry package,<sup>49</sup> whereas the interaction difference density maps and the electrostatic potential maps were obtained using the modified version<sup>50</sup> of the MOLDEN program.<sup>51</sup>

### 3. Results and Discussions

The smallest system that was taken into consideration in our calculations represents a super-cell (SC), consisting of six molecules and atoms (Figure 2). There are 15 possibilities of pair interactions in this arrangement. However, due to symmetry, only nine of those are nonredundant. The results of the interaction energy decomposition for all of the above-mentioned complexes are reported in Table 2. The labeling corresponds to the nomenclature introduced in Figure 2. Careful analysis of the obtained results reveals that there are three important types of interaction leading to the stabilization of the crystal structure. Two of those are the interactions between the sodium cation and the carbanion, and the third is the interaction of Na<sup>+</sup> with the neighboring water molecule. On the other hand the most important destabilizing interactions are due to the electrostatic repulsion of like-charged ions. The interaction energy decomposition reveals that the classical electrostatic interactions of the charge density distributions determine the overall character and strength of the interactions within the studied crystal. The multipole expansion of the first-order electrostatic interaction reported in Table 3 confirms that the main contribution in the case of ionic interactions comes from the charge–charge type interactions, whereas in the case of Na<sup>+</sup>...OH<sub>2</sub> from the charge–dipole interaction. The quantum induction effects included in the delocalization component stabilize the attractive interactions even further. These are, however, to some extent quenched by the Heitler–London exchange repulsion. The determined correlation corrections to the interaction energy clearly indicate that these effects are almost negligible in the case of studied systems. The only substantial contribution to the interaction resulting from the correlation effects comes from the dispersion interactions of the neighboring carbanions, and even in this case it is an order of magnitude smaller than the relevant electrostatic

**TABLE 3: Multipole Expansion of the Electrostatic Interaction Energy Component for Selected Dimers of the 2A System<sup>a</sup>**

	AD	BE	AB(DE)	AE(BD)	BC(EF)
$\epsilon_{el,DMA}^{(1)}$	59.5	36.6	-88.2	-81.5	-26.8
$\epsilon_{el,C-C}^{(1)}$	55.7	36.6	-105.0	-70.5	-5.6
$\epsilon_{el,C-D}^{(1)}$	8.9	0.0	16.6	-11.8	-16.9
$\epsilon_{el,C-Q}^{(1)}$	0.3	0.0	0.2	0.4	-3.7
$\epsilon_{el,D-D}^{(1)}$	-3.8	0.0	0.0	0.0	0.0
$\epsilon_{el,C-O}^{(1)}$	-1.4	0.0	0.0	0.5	-0.6
$\epsilon_{el,D-Q}^{(1)}$	-0.5	0.0	0.0	0.0	0.0
$\epsilon_{el,Q-Q}^{(1)}$	0.3	0.0	0.0	0.0	0.0
$\epsilon_{el,PEN}^{(1)}$	-0.9	0.0	-1.5	1.7	0.6
$\epsilon_{el}^{(10)}$	58.6	36.6	-89.7	-79.8	-26.2

<sup>a</sup> The results were obtained with the 3-21G(d,p) basis set using the distributed atomic multipolar expansion of the charge distributions of monomers. The labels of dimers correspond to the symbols used in Figure 2. The subscripts indicate the type of interaction, where C, D, Q, and O indices stand for charge, dipole, quadrupole, and octupole moments, respectively. All values are in kcal/mol.

interactions. Even though the super-cell structure is rather distant from the bulk crystal and there are no sodium ions at a close distance from each other present in this system, already there are some clues concerning the enigmatic crystal packing. The sodium ion is surrounded by two polar groups of the neighboring carbanions and the water molecule, which is not just the “included solvent” but in fact contributes greatly to the overall stabilization of the super-cell structure. In the actual crystal structure each water molecule is in close proximity to two sodium ions, which makes its function even more important.

The analysis of the results of many-body interaction energy partitioning in the super-cell structure reported in the Table 1 reveals that the nonadditivity is indeed large, since its contribution to the total interaction energy exceeds 14%. It is interesting to note that the basis set extension does not affect the qualitative picture emerging from the results of calculations. Moreover, in the case of Hartree–Fock nonadditive components the basis set extension effects are even smaller, and their values remain practically unaffected by the changes in the quality of the applied basis set. The main contribution to the nonadditivity comes from the repulsive three-body delocalization component, since the many-body exchange effects are negligible and the attractive contribution from the four-body delocalization term is an order



**TABLE 4: Many-Body Partitioning of the Hartree–Fock Interaction Energy for All Studied Systems<sup>a</sup>**

	3-21G(d,p)							6-31G(d,p)			
	SC	2A	2B	2C	4AB	4AC	4BC	SC	2A	2B	2C
$\epsilon_{el}^{(10)}$	−145.0	−162.3	−145.3	−152.2	−144.1	−168.6	−156.8	−139.7	−154.9	−140.2	−146.7
$\epsilon_{el,DMA}^{(1)}$	−147.0	−157.6	−146.6	−152.1				−137.5	−147.3	−137.2	−141.7
$\epsilon_{el,PEN}^{(1)}$	2.0	−4.8	1.3	−0.2				−2.2	−7.6	−3.0	−5.0
$\epsilon_{ex,2}^{HL}$	16.6	33.8	18.2	19.4	16.8	37.1	22.5	16.6	33.9	18.4	19.6
$\epsilon_{ex,3+}^{HL}$	0.0	−0.1	0.0	−0.1	0.0	−0.3	−0.1	0.0	−0.1	0.0	−0.1
$\Delta E_{del,2}^{HF}$	−24.4	−38.2	−25.7	−31.6	−27.2	−48.0	−34.5	−26.4	−41.3	−27.9	−33.9
$\Delta E_{del,3+}^{HF}$	16.5	24.4	17.0	22.6	18.1	33.5	24.8	17.1	25.7	17.8	23.5
$\Delta E^{HF}$	−136.4	−142.4	−135.7	−141.9	−136.3	−146.3	−144.1	−132.4	−136.7	−132.0	−137.6
$\Delta E_2^{HF}$	−152.9	−166.7	−152.7	−164.5	−154.4	−179.5	−168.8	−149.5	−162.3	−149.7	−161.0
$\Delta E_{3+}^{HF}$	16.5	24.3	17.0	22.6	18.1	33.2	24.7	17.1	25.6	17.8	23.4

<sup>a</sup> For the sake of comparison the interaction energy components were divided by the number of unit cells in the structure. The labels of systems are explained in the text. Subscript “+” indicates the sum of all remaining many-body components. All values are in kcal/mol.

of magnitude smaller. The estimated total correlation correction to the interaction energy is totally insignificant, at least at the level of theory applied. The many-body partitioning of the  $\epsilon_{MP}^{(2)}$  term reveals that it is due to a cancellation of additive and nonadditive components, although the respective absolute values of the correlation components are also relatively small. It is interesting to note that the nonadditive components are of the same order of magnitude or even larger than the total two-body contribution. Although the description of the electron correlation effects at the MP2/cc-pVDZ level of theory is rather far from saturation, the basis set extension would probably lead only to the relatively small quantitative changes of the correlation interaction energy components.

The more extensive systems investigated in this work were obtained by translation of the super-cell in the A, B, and C directions, leading to the structures 2A, 2B, and 2C, respectively, shown schematically in Figure 2, and their extensions 4AB, 4AC, and 4BC obtained by translation of structures 2A, 2B, and 2C in the A, B, and C directions. The only type of pair interaction missing in the SC structure and occurring in the 2A and larger systems is the hydrogen bonding between the water molecule and one of the oxygens from the nitro group of the carbanion. This is a typical hydrogen bond, very similar to the one occurring in a water dimer with the  $\Delta E^{HF}$  equal to  $-3.77$  kcal/mol in the 6-31G(d,p) basis set. This contribution, however, to a large extent cancels out with the other two types of repulsive water–carbanion neighboring interactions. The total Hartree–Fock interaction energies of these systems and their many-body partitioning can be found in Table 4. For the sake of comparison the actual values of the interaction energies and their components were divided by the number of unit cells present in the structure. The preliminary conclusions drawn from examination of the interaction energy components of the possible dimeric subsystems were confirmed also in this analysis. The dominating electrostatic character of the interactions persists even if the many-body effects are taken into account. This is mainly due to the fact that the stabilizing two-body delocalization energy  $\Delta E_{del,2}^{HF}$  cancels out to a large extent with the exchange repulsion, which in all studied systems is practically pairwise additive. As a result the destabilizing three-body delocalization interactions  $\Delta E_{del,3+}^{HF}$ , constituting the vast majority of the total nonadditivity of the interactions in all studied systems, become very important. The estimated contribution of the many-body terms varies from 12% to as much as 22% of the total interaction energy.

A better understanding of the origins of changes in the electronic structure of the subsystems of the studied crystal fragment, induced by their mutual interactions, can be derived from the inspection of the interaction difference density maps.

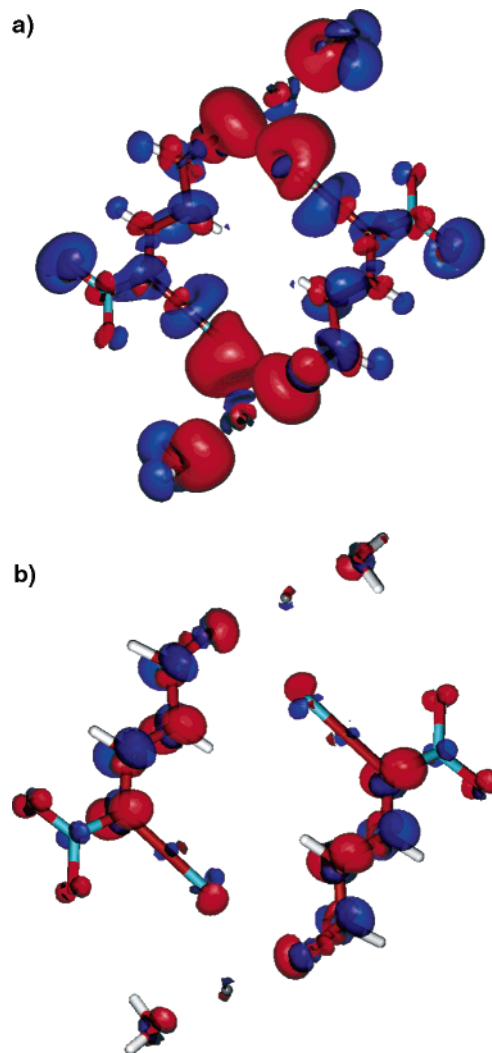


**Figure 3.** Interaction difference density maps of the super-cell system: (a) two-body and (b) three-body. The orientation of the molecular frame is the same as in Figure 2. Red designates an increase of the electron density caused by the two- or three-body intermolecular interactions, whereas blue indicates a related decrease of the electron density. The isodensity contours were plotted for  $\pm 0.001$  electron/bohr<sup>3</sup>.

Such changes were visualized in Figure 3, where the contours of the two-body and the three-body IDDMs obtained at the HF level of theory are plotted for the case of the super-cell system. Since the alterations of the electron density distributions of the interacting subsystems corresponding to the Heitler–London interaction energy components are related only to the small rotations of their orbitals, the visible changes can be attributed

mainly to the delocalization effects. The changes in the electron density distributions of the monomers related to the two-body interactions pictured in Figure 3a indicate the nature of the induced multipole moments. Particularly, a large polarization of the water molecules and the “oxo” and “cyano” groups of the carbanion can be seen, which results in a large electron density increase in the immediate neighborhood of the sodium ions. In fact the electronic population analyses conducted at the RHF/cc-pVDZ level of theory show that the charge transfer to the cations is indeed substantial, as the net charge of the sodium ions obtained applying the Mulliken<sup>52</sup> and Löwdin<sup>53</sup> schemes equals 0.62e and 0.16e(!), respectively. This fact also to some extent explains why the clustering of the sodium ions in the crystal structure was possible. On the other hand, the analysis of the three-body IDDM shown in Figure 3b reveals that the three-body delocalization interactions, which are the major nonadditive components in all studied systems, seem to be related mainly to the resonance effects within the electronic structure of the carbanions. The calculations carried out for the isolated carbanion indicate that of all the possible resonance structures, the simplistic diagram shown in Figure 1 is the most consistent with the ab initio results, even though the excess electron is fairly delocalized throughout the entire structure of the carbanion. Such a conclusion is based on the analysis of the calculated electrostatic potential map (Figure 1) and the results of the Mulliken and Löwdin population analyses. The pair interactions of the carbanion with the two neighboring sodium ions result in a substantial charge transfer to the cations, which leads to the considerable modifications of its electronic structure (Figure 3a). Hence a straightforward interpretation of the electron density changes that are visible in Figure 3b would be a partial restoration of the resonance structure shown in Figure 1 due to the three-body delocalization effects, i.e., when the carbanion interactions with both neighboring sodium ions are properly accounted for. This effect, however, destabilizes the crystal structure noticeably.

#### 4. Conclusions

The hybrid variation–perturbation decomposition of the interaction energy has been employed in order to analyze the physical nature of interactions in the ionic 3-pentenitrile, 2-nitro-5-oxo, ion(−1), sodium crystal, which can be regarded as a model for a large group of aromatic quaternary nitrogen salts. Although only a relatively small fragment of the crystal structure could be investigated, and the studied systems are rather distant from the bulk crystal, the reported results provide a reasonable explanation of the analyzed crystal packing. In the crystal structure each sodium ion is surrounded by two polar groups of the neighboring carbanions and the water molecule, and all of these interactions contribute significantly to the overall stabilization of the crystal structure. The strong favorable interaction between the water molecule and the sodium ion and the substantial charge transfer from the carbanions balance out the destabilizing sodium–sodium ion repulsion. One concludes that the water molecule plays an important role in stabilizing the crystal structure. Moreover, each water molecule interacts with two sodium ions, which makes its presence even more important. Such conclusions are in line with well-established knowledge in the area of hydrated ionic crystals that water molecules play an important, although very subtle, role in the hydrated crystal stability and their phase transitions.<sup>19</sup>

It is safe to assume that the majority of the cohesion energy of the studied crystal comes from the charge–charge and charge–dipole electrostatic interactions. However, due to the

fact that the two-body delocalization and exchange effects cancel each other out to a large extent, the resulting net stabilization also depends heavily on the contributions from the nonadditive delocalization components. This concerns particularly the destabilizing three-body delocalization interactions  $\Delta E_{del,3}^{HF}$ , which constitute the vast majority of the total nonadditivity of the interactions. The analysis of the three-body interaction difference density map of the super-cell system reveals that the aforementioned interactions are related mainly to the resonance effects in the electronic structure of the carbanions. The estimated overall contribution of the many-body terms to the total interaction energy ranging from 12% to 22%, depending on the studied system, indicates a significant nonadditivity of the interactions and need for their inclusion and proper representation in a simpler theoretical models.

**Acknowledgment.** The authors thank Dr. Jerome Karle for helpful comments and discussions and Dr. Glake Hill for reading and commenting on the manuscript. J.L. is grateful for the Distinguished Faculty Fellow 2003 ONR-ASEE award. This work was facilitated in part by the NSF grant No. 9805465 & 9706268, ONR grant No. N00014-98-1-0592, the Army High Performance Computing Research Center under the auspices of the Department of the Army, Army Research Laboratory cooperative agreement number DAAH04-95-2-0003/contract number DAAH04-95-C-0008, and Wrocław University of Technology. This work does not necessarily reflect the policy of the government, and no official endorsement should be inferred. We would like to thank the Mississippi Center for Supercomputing Research, and Wrocław Supercomputing and Networking Center for a generous allotment of computer time.

#### References and Notes

- (1) Lommerse, J. P. M.; Motherwell, W. D. S.; Ammon, H. L.; Dunitz, J. D.; Gavezzotti, A.; Hofmann, D. W. M.; Leusen, F. J. J.; Mooij, W. T. M.; Price, S. L.; Schweizer, B.; Schmidt, M. U.; van Eijck, B. P.; Verwer, P.; Williams, D. E. *Acta Crystallogr. B* **2000**, *56*, 697.
- (2) Motherwell, W. D. S.; Ammon, H. L.; Dunitz, J. D.; Dzyabchenko, A.; Erk, P.; Gavezzotti, A.; Hofmann, D. W. M.; Leusen, F. J. J.; Lommerse, J. P. M.; Mooij, W. T. M.; Price, S. L.; Scheraga, H.; Schweizer, B.; Schmidt, M. U.; van Eijck, B. P.; Verwer, P.; Williams, D. E. *Acta Crystallogr. B* **2002**, *58*, 647.
- (3) Dunitz, J. D. *Chem. Commun.* **2003**, *1*, 545.
- (4) Sokalski, W. A.; Lowrey, A. H.; Roszak, S.; Lewchenko, V.; Blaisdell, J.; Hariharan, P. C.; Kaufman, J. J. *J. Comput. Chem.* **1986**, *7*, 693.
- (5) Cabalero-Lago, E. M.; Rios, M. A. *J. Chem. Phys.* **1999**, *110*, 6782.
- (6) Mitchell, J. B. O.; Price, S. L. *J. Phys. Chem. A* **2000**, *104*, 10958.
- (7) Mitchell, J. B. O.; Price, S. L.; Leslie, M.; Buttar, D.; Roberts, R. *J. J. Phys. Chem. A* **2001**, *105*, 9961.
- (8) van Duijneveldt-van de Rijdt, J. G. C. M.; Mooij, W. T. M.; van Duijneveldt, F. B. *Phys. Chem. Chem. Phys.* **2003**, *5*, 1169.
- (9) Haies, I. C.; Stone, A. J. *Mol. Phys.* **1984**, *53*, 83.
- (10) Jeziorski, B.; Moszynski, R.; Szalewicz, K. *Chem. Rev.* **1994**, *94*, 1887.
- (11) Gutowski, M.; van Duijneveldt, F. B.; Chalasinski, G.; Piela, L. *Mol. Phys.* **1987**, *61*, 233.
- (12) Sokalski, W. A.; Roszak, S.; Pecul, K. *Chem. Phys. Lett.* **1988**, *153*, 153.
- (13) Cybulski, S. M.; Chałasiński, G.; Moszyński, R. *J. Chem. Phys.* **1990**, *92*, 4357.
- (14) Gora, R. W.; Bartkowiak, W.; Roszak, S.; Leszczynski, J. *J. Chem. Phys.* **2002**, *117*, 1031.
- (15) Gora, R. W.; Bartkowiak, W.; Roszak, S.; Leszczynski, J. *J. Chem. Phys.* **2004**, *120*, 2802.
- (16) Reinheimer, J. D.; Mayle, L. L.; Dolnikowski, G. G.; Gerig, J. T. *J. Org. Chem.* **1980**, *45*, 3097.
- (17) Reinheimer, J. D.; Sourbatis, N.; Lavalley, R. L.; Goodwin, D.; Gould, G. L. *Can. J. Chem.* **1984**, *62*, 1120.
- (18) Haynes, L. W.; Pett, V. B. Manuscript in preparation.
- (19) Wells, A. F. *Structural Inorganic Chemistry*; Oxford University Press, 1984.

- (20) Dedonder-Lardeux, C.; Gregoire, G.; Jouvet, C.; Martrenchard, S.; Solgadi, D. *Chem. Rev.* **2000**, *100*, 4023.
- (21) Ayala, R.; Martinez, J. M.; Pappalardo, R. R.; Sanchez Marcos, E. *J. Phys. Chem. A* **2000**, *104*, 2799.
- (22) Dykstra, C. E. *J. Chem. Phys.* **1998**, *108*, 6619.
- (23) Thompson, M. A. *J. Phys. Chem.* **1996**, *100*, 14492.
- (24) Elrod, M. J.; Saykally, R. J. *Chem. Rev.* **1994**, *94*, 1975.
- (25) Hankins, D.; Moskowitz, J. W.; Stillinger, F. H. *J. Chem. Phys.* **1970**, *53*, 4544.
- (26) Xantheas, S. S. *J. Chem. Phys.* **1994**, *100*, 7523.
- (27) Chen, W.; Gordon, M. S. *J. Phys. Chem.* **1996**, *100*, 14316.
- (28) Møller, C.; Plesset, M. S. *Phys. Rev.* **1934**, *46*, 618.
- (29) Wells, B. H.; Wilson, S. *Chem. Phys. Lett.* **1983**, *101*, 429.
- (30) Mierzwicki, K.; Latajka, Z. *Chem. Phys. Lett.* **2003**, *380*, 654.
- (31) Chałasiński, G.; Szczęśniak, M. M. *Mol. Phys.* **1988**, *63*, 205.
- (32) Chałasiński, G.; Szczęśniak, M. M. *Chem. Rev.* **1994**, *94*, 1723.
- (33) Jeziorski, B.; Bulski, M.; Piela, L. *Int. J. Quantum Chem.* **1976**, *10*, 281.
- (34) Löwdin, P. O. *Adv. Phys.* **1956**, *5*, 1.
- (35) Stone, A. J. *Chem. Phys. Lett.* **1981**, *83*, 233.
- (36) Stone, A. J.; Alderton, M. *Mol. Phys.* **1985**, *56*, 1047.
- (37) Sokalski, W. A.; Poirier, R. A. *Chem. Phys. Lett.* **1983**, *98*, 86.
- (38) Sokalski, W. A.; Sawaryn, A. *J. Chem. Phys.* **1987**, *87*, 526.
- (39) Gutowski, M.; Piela, L. *Mol. Phys.* **1988**, *64*, 943.
- (40) Jeziorski, B.; van Hemert, M. C. *Mol. Phys.* **1976**, *31*, 713.
- (41) Moszyński, R.; Rybak, S.; Cybulski, S.; Chałasiński, G. *Chem. Phys. Lett.* **1990**, *166*, 609.
- (42) Binkley, J. S.; Pople, J. A.; Hehre, W. J. *J. Am. Chem. Soc.* **1980**, *102*, 939.
- (43) Gordon, M. S.; Binkley, J. S.; Pople, J. A.; Pietro, W. J.; Hehre, W. J. *J. Am. Chem. Soc.* **1983**, *104*, 2797.
- (44) Pietro, W. J.; Francl, M. M.; Hehre, W. J.; DeFrees, D. J.; Pople, J. A.; Binkley, J. S. *J. Am. Chem. Soc.* **1982**, *104*, 5039.
- (45) Hehre, W. J.; Ditchfield, R.; Pople, J. A. *J. Chem. Phys.* **1972**, *56*, 2257.
- (46) Francl, M. M.; Petro, W. J.; Hehre, W. J.; Binkley, J. S.; Gordon, M. S.; DeFrees, D. J.; Pople, J. A. *J. Chem. Phys.* **1982**, *77*, 3654.
- (47) Hariharan, P. C.; Pople, J. A. *Theor. Chim. Acta* **1973**, *28*, 213.
- (48) Gora, R. W. *EDS v2.1.2 package*; Wrocław, Poland, Jackson, MS, 1998–2003.
- (49) Schmidt, M. W.; Baldridge, K. K.; Boatz, J. A.; Elbert, S. T.; Gordon, M. S.; Jensen, J. H.; Koseki, S.; Matsunaga, N.; Nguyen, K. A.; Su, S. J.; Windus, T. L.; Dupuis, M.; Montgomery, J. A. *J. Comput. Chem.* **1993**, *14*, 1347.
- (50) Gora, R. W. *DENDIF v2.1.1 package*; Wrocław, Poland, Jackson, MS, 2001–2003.
- (51) Schaftenaar, G.; Noordik, J. H. *J. Comput.-Aided Mol. Des.* **2000**, *14*, 123.
- (52) Mulliken, R. S. *J. Chem. Phys.* **1955**, *23*, 1833.
- (53) Löwdin, P. O. *Adv. Chem. Phys.* **1970**, *5*, 185.